Monthly Notices
of the
ROYAL ASTRONOMICAL SOCIETY

MNRAS **445,** 3105–3114 (2014) doi:10.1093/mnras/stu1905

Flux-density spectral analysis for several pulsars and two newly identified gigahertz-peaked spectra pulsars

M. Dembska,[1,2]★ J. Kijak,[1] A. Jessner,[3] W. Lewandowski,[1] B. Bhattacharyya[4] and Y. Gupta[5]

[1]*Kepler Institute of Astronomy, University of Zielona Góra, Lubuska 2, PL-65-265 Zielona Góra, Poland*
[2]*German Aerospace Center, Institute for Space Systems, Robert Hooke Str. 7, D-28359 Bremen, Germany*
[3]*Max-Planck-Institut für Radioastronomie, Auf dem Hügel 69, D-53121 Bonn, Germany*
[4]*Inter-University Centre for Astronomy, and Astrophysics, Pune 411007, India*
[5]*National Centre for Radio Astrophysics, Pune University Campus, Postbag 3, India 411007*

Accepted 2014 September 11. Received 2014 September 11; in original form 2014 May 20

ABSTRACT

In this paper, we present results from flux-density measurements for 21 pulsars over a wide frequency range, using the Giant Metrewave Radio Telescope (GMRT) and the Effelsberg telescope. Our sample was a set of mostly newly discovered pulsars from the selection of candidates for gigahertz-peaked spectra (GPS) pulsars. Using the results of our observations along with previously published data, we identify two new GPS pulsars. One of them, PSR J1740+1000, with dispersion measure (DM) of 24 pc cm^{-3}, is the first GPS pulsar with such a low DM value. We also selected several strong candidates for objects with high-frequency turnover in their spectra, which require further investigation. We also revisit our source selection criteria for future searches for GPS pulsars.

Key words: pulsars: general – pulsars: individual: J1740+1000 – pulsars: individual: J1852−0635.

1 INTRODUCTION

Of the about 2000 known pulsars, only around 400 have measured flux-density spectra. For most of these cases, the flux-density spectra can be described using either a power law of the form

$$S(\nu) = d\nu^{\xi}, \tag{1}$$

where ν denotes observing frequency, with a negative spectral index ξ of about -1.8, or a combination of two power laws

$$S(\nu) = \begin{cases} c_1\nu^{\xi_1} : \nu \leqslant \nu_{\rm b} \\ c_2\nu^{\xi_2} : \nu > \nu_{\rm b} \end{cases} \tag{2}$$

with spectral indices ξ_1 and ξ_2 having average values of -0.9 and -2.2, respectively, with a break frequency $\nu_{\rm b}$, which is typically around 1.5 GHz (Maron et al. 2000). The population of pulsars with such a break in the spectra is about 10 per cent of the sample analysed by Maron et al. (2000), and it is usually assumed that both ξ_1 and ξ_2 are negative, with ξ_2 being steeper than ξ_1. For pulsars that can be observed at low frequencies (i.e. about 100–600 MHz), a low-frequency turnover is observed in the spectra (Sieber 1973; Lorimer et al. 1995). In some cases, positive spectral indices have also been observed between 400 and 1600 MHz (Lorimer et al. 1995).

Kijak, Gupta & Krzeszowski (2007) showed the first direct evidence of a high-frequency turnover in radio pulsar spectra using multifrequency flux measurements for candidates chosen from objects that showed a decrease of flux density at frequencies below 1 GHz. The frequency at which such a spectrum shows the maximum flux is called the peak frequency $\nu_{\rm p}$. Later, Kijak et al. (2011b) presented a new class of objects, called gigahertz-peaked spectra (GPS) pulsars. These sources exhibit a turnover in their spectra at high frequencies with $\nu_{\rm p}$ about 1 GHz or above. To analyse the shapes of GPS, we use a function

$$S(\nu) = 10^{ax^2+bx+c}, \quad x \equiv \log_{10}\nu, \tag{3}$$

previously proposed for similar studies of pulsar spectra with turnover at low frequencies (Kuzmin & Losovsky 2001).

GPS pulsars have been demonstrated to be relatively young objects, and have high dispersion measures ($DM \geq 150$ pc cm^{-3}, Kijak et al. 2011a, b). They usually adjoin interesting and often dense objects in their vicinity, for example, H II regions and compact pulsar wind nebulae (PWNe). In addition, it seems that they are coincident with known but sometimes unidentified X-ray sources from the Third Energetic Gamma-Ray Experiment Telescope (EGRET) Catalogue or High Energy Stereoscopic System (HESS) observations. This, in turn, suggests that the high-frequency turnover is a result of the environmental conditions around neutron stars and/or the physical properties of the interstellar medium. Although GPS

★ E-mail: marta.dembska@dlr.de

pulsars represent the smallest group of radio pulsar spectra types today, Bates, Lorimer & Verbiest (2013) estimate that the number of such sources might be as much as 10 per cent of the whole pulsar population. It is obvious that without a more extensive sample of these sources, it is not possible to constrain reliably any statistics of their properties.

The evolution of the spectrum of PSR B1259−63 with orbital phase can be treated as a key factor to define physical mechanisms that could potentially be responsible for the GPS phenomenon. The object is in a unique binary system with a massive (10 $M_{\odot}$), main-sequence, Be star LS2883 with a radius of 6 $R_{\odot}$. PSR B1259−63 is a middle-aged pulsar (330 kyr) with a relatively short period of 48 ms. Its average DM is about 147 pc cm^{-3}. The system is an eccentric binary ($e = 0.87$) with an orbital period of 3.4 yr and a projected semimajor axis, $a\sin i$, of 1300 light seconds (2.6 au). Kijak et al. (2011a) used published data (Johnston et al. 1999, 2005; Connors et al. 2002) to show that at various orbital phases of the binary, the radio spectrum of PSR B1259−63 mimics that of pulsars with the GPS. They also presented evidence for the evolution of the spectrum of the pulsar due to its orbital motion, along with the peak frequency dependence on the orbital phase. Kijak et al. (2011a) proposed two possible causes of the observed variation in the spectra: free–free absorption in the stellar wind and cyclotron resonance in the magnetic field associated with a disc of the Be star. This observed evolution of the PSR B1259−63 spectrum seems to be the most convincing proof for an environmental origin of the GPS phenomenon.

Kijak et al. (2013) studied the radio spectra of two magnetars PSRs J1550−5418 and J1622−4950, which clearly show turnover at frequencies of a few GHz. Both these magnetars are associated with supernova remnants (SNRs), and thus are surrounded by a hot, ionized gas, which could be responsible for the free–free absorption of radio waves. Kijak et al. (2013) concluded that the GPS feature in the radio spectra of magnetars could be caused by external factors, in the same way as in the environment of GPS pulsars.

Recently, Allen et al. (2013) presented the spectrum of a newly discovered pulsar PSR J2007+2722, which shows a high-frequency turnover (see their table 5). It is possible that PSR J2007+2722 is a young pulsar that was born with a relatively weak magnetic field and with a birth period longer than is usually assumed. In this case, with its $DM = 127$ pc cm^{-3}, the object seems to be similar to other GPS pulsars. The distance of 5.4 kpc, corresponding to the DM value, could be the reason why there has been no mention of a SNR or a PWN around PSR J2007+2722.

In this paper, we present flux measurements for 21 pulsars, resulting from observations at both low and high frequencies. The sample was chosen from objects suspected to be GPS pulsars. The results of our observations allow us to indicate several new sources showing GPS properties, and also strong GPS candidates. We conclude with a review of the source selection criteria for future searches for GPS pulsars.

2 OBSERVATIONS AND RESULTS

In this paper, we present the flux-density measurements collected during two observing projects. We were able to successfully measure the flux densities of 12 pulsars at 610 MHz and to estimate upper limits for another four pulsars, during observations in 2010 May with the Giant Metrewave Radio Telescope (GMRT; near Pune, India); see also Kijak et al. (2011c). We also used the 100-m Effelsberg Radio Telescope for flux-density measurements of 11 pulsars at 2.6, 4.85 and 8.35 GHz in 2012 November. The main purpose of these observations was to find more pulsars showing GPS.

We chose the sources to be observed with the GMRT from a set of newly discovered pulsars with periods between 0.1 and 2.0 s, whose flux-density measurements at 1.4 GHz are available in the Australia Telescope National Facility (ATNF) pulsar catalogue.[1] The observations were conducted in the phased array mode of the GMRT (Gupta 2000), with the available 16-MHz bandwidth divided into 256 channels, and using a sampling rate of 0.512 ms. The typical integration time was about 30 min (for more details, see Kijak et al. 2011b).

For the Effelsberg observing project, we selected pulsars based on our GMRT observations, along with data from the ATNF catalogue and from Maron et al. (2000). We selected objects that appeared to have a flat spectrum or a positive spectral index below a frequency of 1 GHz. To ascertain the full shape of the spectrum, it was necessary to measure the flux densities at frequencies above 2 GHz. For these observations, we used the secondary focus receivers (with cooled HEMT amplifiers) with bandwidths of 100 MHz at 2.6 GHz, 500 MHz at 4.85 GHz and 1100 MHz at 8.35 GHz. These receivers provided circularly polarized left-hand circular (LHC) and right-hand circular (RHC) signals, digitized and independently sampled with 1024 bins per period, and synchronously folded using the topocentric pulsar rotational period (Jessner 1996). The typical integration time was around 20–25 min. The observations were intensity calibrated by the use of a noise diode and known continuum radio sources (NGC 7027, 3C 286, 3C 345).

Table 1 combines the weighted means of all flux-density measurements and their uncertainties for our sample of 21 pulsars, acquired at different frequencies with the GMRT and the Effelsberg observing projects. Most sources in our sample have high DMs and hence the flux-density variations caused by interstellar scintillations should be minimal. Nevertheless, observations at each frequency (with a few exceptions) were conducted at two to three different epochs to give us reliable estimates of the average flux and its uncertainties, which are used to construct the spectra for these pulsars, in combination with flux-density data available from the literature. In Table 1, we also present other basic parameters of these pulsars, such as age, DM and period.

3 SPECTRA

We constructed radio spectra for the pulsars listed in Table 1, using the flux-density measurements derived from the above observing projects along with data taken from the literature (Lorimer et al. 1995; Maron et al. 2000; Kijak et al. 2007, 2011b) and the ATNF catalogue. We divided our sources into groups depending on the morphological type of their spectra. The first two objects presented below can be classified as new GPS pulsars. Three other sources were revealed to be strong candidates for pulsars with high-frequency turnover in their spectra, or possibly – as in the case of PSRs B1811+40 and B1904+06 – pulsars with broken spectra. A third group contains all the remaining sources, which show power-law spectra (sometimes with a potential break or low-frequency turnover feature) together with the objects whose morphological types of spectra cannot be identified because they have their flux density measured at only one or two frequencies.

[1] http://www.atnf.csiro.au/research/pulsar/psrcat/ (Manchester et al. 2005)

Table 1. The weighted means of all flux-density measurements and their uncertainties for our sample of 21 pulsars are presented. Results from observations conducted in 2010 using the GMRT in phased array mode at 610 MHz are marked as S_{610}; those using the Effelsberg telescope in 2012 at three frequencies, 2.6, 4.85 and 8.35 GHz, are denoted by S_{2600}, S_{4850} and S_{8350}, respectively. The total number of observations at each frequency is given in parentheses; the symbol < denotes an upper limit. Flux-density measurements from observations in 2008 are given in the table notes. Data collected in 2008 and 2010 were partially published (see Kijak et al. 2011c). Where possible, the value of ξ, the power index fitted to the spectra (using our data in combination with previously published data for individual pulsars), along with the reduced χ^2, is given in the last two columns. There are no errors in the fits for ξ for degenerate cases where the number of data points equals the number of parameters.

Pulsar	Period (s)	DM (pc cm^{-3})	Age (kyr)	S_{610} (mJy)	S_{2600} (mJy)	S_{4850} (mJy)	S_{8350} (mJy)	ξ	χ^2
J1705−3950	0.319	207	83.4	1.2 ± 0.1 (3)				0.3	–
J1723−3659	0.203	254	401	2.9 ± 0.2 (2)				−0.8	–
J1739−3023	0.114	170	159	2.7 ± 0.2 (2)				−1.2	–
J1740+1000	0.154	24	114		2.0 ± 0.7 (2)	1.6 ± 0.1 (2)	0.344 ± 0.014 (2)		
J1744−3130	1.070	193	796	1.7 ± 0.3 (2)				−1.1	–
J1751−3323	0.548	297	984	1.7 ± 0.3 (2)				−0.32	–
J1755−2521	1.180	252	207	<1.0 (2)					
B1811+40 (J1813+4013)	0.931	42	5790		0.185 ± 0.036 (1)			−1.2 ± 0.1	0.9
J1812−2102	1.220	547	811	<2.7 (2)	0.38 ± 0.07 (3)	0.117 ± 0.024 (3)		−2.0 ± 0.1	0.08
J1834−0731	0.513	295	140	<1.6 (3)	0.406 ± 0.009 (3)	0.216 ± 0.064 (3)		−1.41 ± 0.14	0.6
J1835−1020	0.302	114	810	3.6 ± 1.0 (3)				−0.8	–
J1841−0345	0.204	194	55.9	3.5 ± 2.0 (2)	0.979 ± 0.015 (2)	0.568 ± 0.009 (1)		−0.85 ± 0.04	1.4
J1842−0905	0.345	343	520	2.2 ± 0.3 (2)				−1.2	–
J1852−0635[a]	0.524	171	567	7.0 ± 0.7 (3)	7.0 ± 0.2 (3)	4.686 ± 0.044 (3)	1.83 ± 0.14 (3)		
J1857+0143	0.140	249	71	<1.0 (1)					
J1901+0510	0.615	429	313	3.4 ± 1.5 (2)				−1.8	–
B1903+07 (J1905+0709)	0.648	245	2080		0.59 ± 0.12 (2)			−1.57 ± 0.14	4.2
B1904+06 (J1906+0641)	0.267	473	1980		1.234 ± 0.042 (1)			−0.94 ± 0.18	4.5
J1905+0616[b]	0.990	256	116	2.4 ± 0.5 (1)	0.27 ± 0.01 (3)	0.203 ± 0.023 (3)		−0.88 ± 0.25	4.5
J1910+0728	0.325	284	621	2.4 ± 0.5 (2)	0.647 ± 0.034			−0.70 ± 0.25	3
B1916+14 (J1918+1444)	1.180	27	88.1		2.131 ± 0.019 (1)			−0.21 ± 0.24	0.3

Note: [a] $S_{1170}^{2008} = 9.0 \pm 0.5$ (2).
[b] $S_{610}^{2008} = 2.1 \pm 0.6$ (1) and $S_{1170} = 0.4 \pm 0.1$ (2).

Figs 1–5 show graphical representations of these spectra. Open symbols denote new flux-density measurements that resulted from our observing projects, whereas the previously published data are marked with black dots. Table 1 also shows the power-law spectral indices fitted to some of the presented spectra. The spectral fits to the data were carried out using an implementation of the non-linear least-squares Levenberg–Marquardt algorithm.

3.1 Newly identified GPS pulsars

PSRs J1740+1000 and J1852−0635 have been identified as new pulsars with GPS. In Figs 1 and 2, we present their spectra along with our fits to the data using the function presented in equation (3).

J1740+1000

Kijak et al. (2011b) presented flux measurements of PSR J1740+1000 at frequencies of 610 and 1170 MHz, carried out with the GMRT in phased array mode. The authors were however unable to detect the pulsar during their first attempt at high frequency observations using Effelsberg telescope due to an erroneous ephemeris. New measurements marked as open circles are presented in Fig. 1, along with previous results. One can note that the flux density at 1170 MHz, derived from a previous observing

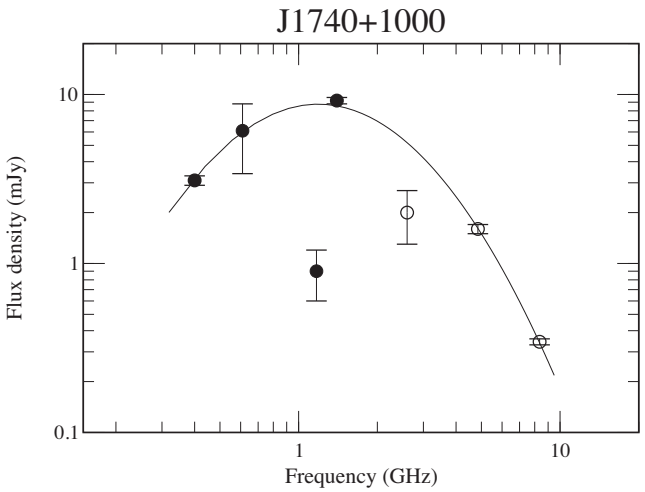

Figure 1. Spectrum of PSR J1740+1000. Open circles denote our observations conducted in 2012, whereas data points marked with black dots are taken from McLaughlin et al. (2002) and Kijak et al. (2011b). The curve represents our fit to the data using the function given in equation (3). The flux density measured at 1070 MHz was excluded from the fitting procedure. Fitted parameters are $a = -1.97 \pm 0.17$, $b = 0.29 \pm 0.13$ and $c = 0.93 \pm 0.05$, with reduced $\chi^2 = 7.8$.

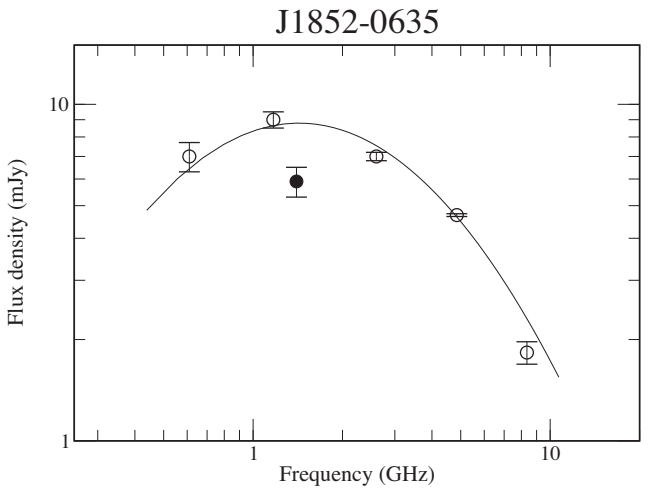

Figure 2. Spectrum of PSR J1852−0635. Open circles denote results from our observations conducted in 2008 and 2010 (at 1070 and 610 MHz, respectively; see also Kijak et al. 2011c) and in 2012 (at 2.6, 4.85 and 8.35 GHz), whereas the black dots denote data from the ATNF catalogue. The curve represents our fits to the data using the function presented in equation (3). The flux density measured at 1.4 GHz was excluded from the fitting procedure. Fitted parameters are $a = -0.99 \pm 0.28$, $b = 0.30 \pm 0.26$ and $c = 0.92 \pm 0.01$, with reduced $\chi^2 = 10.8$.

project (see Kijak et al. 2011b), appears to be substantially smaller than values obtained at neighbouring frequencies – this is possibly due to interstellar scintillations. Regardless of the reason causing the decrease of flux density at 1070 MHz, new observations appear to be sufficient to identify the PSR J1740+1000 spectrum as a GPS-type.

J1852−0635

PSR J1852−0635, which is shown to have a positive spectral index at frequencies below 1 GHz (Kijak et al. 2011c), seemed to be a strong candidate for a GPS pulsar, as confirmed by our new results. Moreover, it is a relatively young object with a high DM, as is typical of most of the GPS pulsars. To the best of our knowledge, there are no radio or high-frequency observations that would prove that this object has any type of peculiar environment, but we cannot rule out this possibility.

In Fig. 2, we present the spectrum of PSR J1852+0635. It seems to be obvious that we are dealing with a GPS-type spectrum. However, the object is a potential candidate for a pulsar with spectra described using the model presented in Löhmer et al. (2008). Thus, we attempted to fit three different functions that had been proposed in the literature, where

$$S(\nu) = \frac{S_0}{1 + (2\pi\nu\tau)^2} \tag{4}$$

and

$$S(\nu) = S_0[1 + (2\pi\nu\tau)^2]^{n-1} \mathrm{e}^{-\mathrm{i}(n-1)\,atan(2\pi\nu\tau)} \tag{5}$$

from Löhmer et al. (2008) are based on a nano-shot emission model. We also considered the empirical function presented in equation (3). Parameters were as follows: $S_0 = 8.7 \pm 0.4$ Jy, $\tau = 0.03 \pm 0.003$ ns, $\chi^2 = 7.9$ for the function presented in equation (4); $S_0 = 404 \pm 13$ Jy, $\tau = 0.038 \pm 0.005$ ns, $\chi^2 = 15.4$ for the function presented in equation (5); $a = -0.99 \pm 0.28$, $b = 0.30 \pm 0.26$, $c = 0.92 \pm 0.01$, $\chi^2 = 10.8$ for the function presented in equation (3). For equation (4), we used a simplex fit procedure, and a Levenberg–Marquardt method was found to be advantageous for equations (3) and (5).

The simple function presented in equation (4) provided the best fit with a nano-shot time-scale of about 30 ps, which is only 10 per cent of what was found for typical pulsars by Löhmer et al. (2008). Alternative equations (3) and (5) gave slightly worse agreement with the data, but generally speaking we find that these three functions match the data quite well within the measured frequency interval. Only at frequencies above 20 GHz, can we expect to be able to differentiate between them, with equations (4) and (3) being steeper than equation (5). All fits predict an average flux density of about 0.5–0.8 mJy.

3.2 Candidates for GPS pulsars

Fig. 3 presents the spectra of PSRs J1705−3950, J1812−2102 and J1834−0731, which can be considered good GPS candidates. New measurements points (open circles) along with the data from the ATNF catalogue (black dots) show a negative spectral index at frequency ranges above 1 GHz for these objects.

PSR J1705−3950, while having flux measurements at only two frequencies, seems to be a strong GPS candidate because it clearly shows a moderately high positive spectral index at frequencies close to 1 GHz. The spectra of PSRs J1755−2521 and J1857+0134 (not presented in Fig. 3) are similar to the spectrum of PSR J1705−3950, although in those cases we have only one flux measurement and one upper limit (see Table 1). Nevertheless, these two objects can also be considered good GPS candidates that deserve further investigation.

In the cases of PSRs J1812−2102 and J1834−0731, from a consideration of the level of the upper limit at 610 MHz and flux-density measurements at higher frequencies (see Fig. 3), it appears that at frequencies below 1 GHz their spectra might be flat or even exhibit a positive spectral index. Moreover, both objects are relatively young, and have high DMs, which makes them similar to other GPS pulsars. However, it definitely requires further investigation to decide whether we are dealing with cases of turnover or a broken type of spectra. Table 1 presents the spectral indices fitted to high-frequency flux values for these two pulsars (excluding data points that are upper limits): the values of −2.0 and −1.41 seem to indicate regular steep spectra. However, it was shown by Kijak et al. (2011b) that, in the high-frequency range, most of the verified GPS pulsars behave like normal spectra pulsars.

3.3 Other pulsars

Here, we present the spectra of pulsars chosen from the remaining 16 objects in our sample. For those with four or more observing points, there is a strong suggestion that their spectra do not show any signs of GPS. As for the spectra of the remaining objects, it was impossible to properly classify them because of the deficiencies of the flux measurements.

The spectra for seven of these remaining 16 pulsars from Table 1 are presented in Figs 4 and 5. For these objects, we are probably dealing with a single power-law spectrum (the fits are presented along with data points). However, the spectra of PSRs B1811+40 and B1904+06 presented in Fig. 5 are potential candidates for broken spectra type with break frequencies 700 MHz and 2.3 GHz, respectively.

The data for PSR B1916+14, as in the case of PSR J1852−0635, were matched to the three different functions, and we obtained reasonable fits with the following parameters: $S_0 = 1.9 \pm 0.27$ Jy, $\tau = 0.1 \pm 0.03$ ns, $\chi^2 = 11.9$ for the function presented in equation

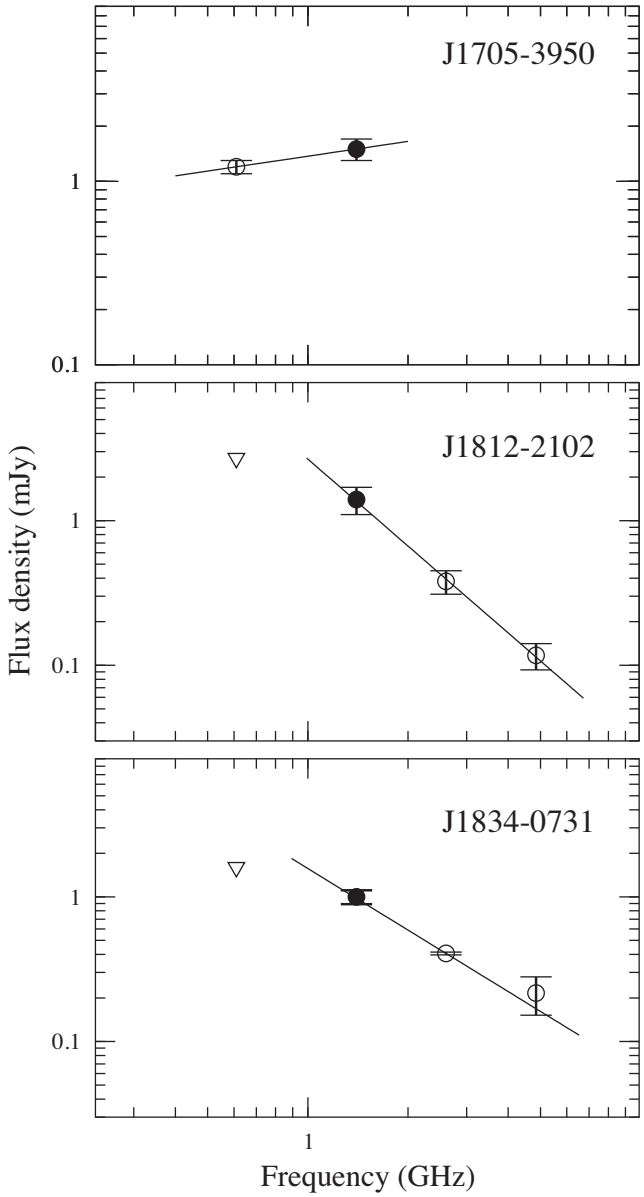

Figure 3. Radio spectra of PSRs J1705−3950, J1812−2102 and J1834−0731. Open symbols denote our observations conducted in 2010 (610 MHz) and 2012 (2.6 and 4.85 GHz), whereas black dots denote data from the ATNF catalogue. Triangles are upper limits. The straight lines represent our fits to the data using the power-law function (upper limits were excluded from the fitting procedure).

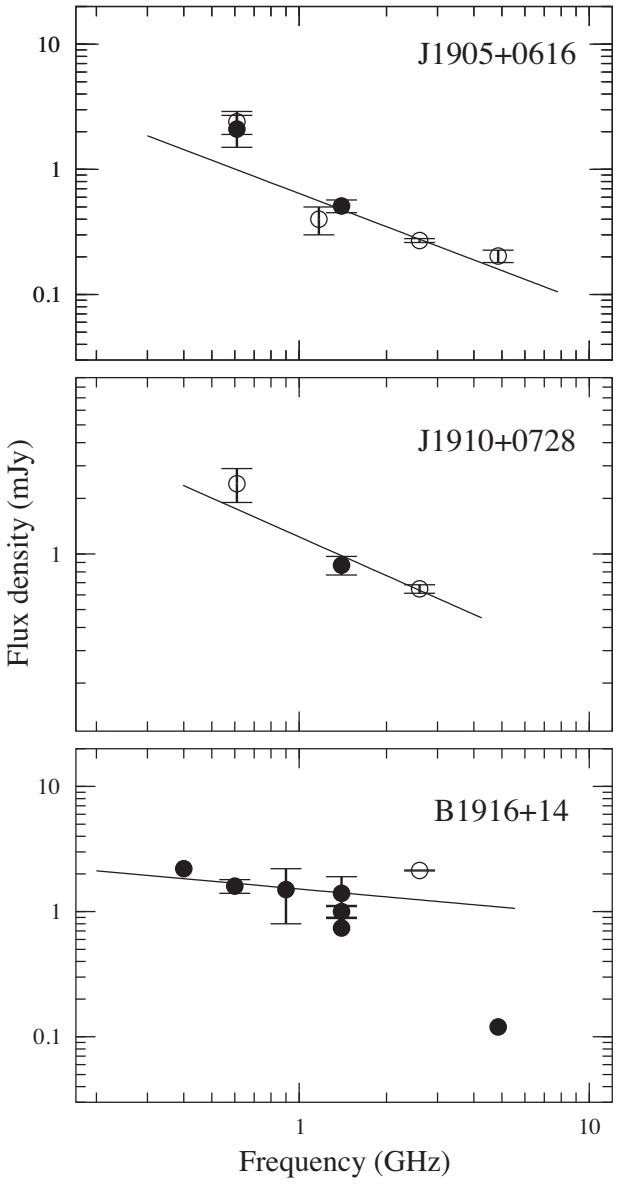

Figure 4. Radio spectra of three pulsars: PSRs J1905+0616, J1910+0728 and B1916+14. Open circles denote our observations conducted in 2008 and 2010 (1070 and 610 MHz, respectively) and in 2012 (2.6 and 4.85 GHz), whereas the black dots denote data from Maron et al. (2000). The straight lines represent our fits to the data using a power-law function (in the case of PSR B1916+14, the marginal data point was excluded from the fitting procedure). The resulting spectral indices are presented in Table 1.

(4); $S_0 = 202 \pm 303$ Jy, $\tau = 0.074 \pm 0.02$ ns, $\chi^2 = 13.5$ for the function presented in equation (5); $a = -1 \pm 0.3, b = -0.64 \pm 0.08$ $c = 0.13 \pm 0.022$, $\chi^2 = 10.7$ for the function presented in equation (3). Again, the fits only begin to diverge significantly above 20 GHz, but here average fluxes of the order of μJy are to be expected, which will require a larger and more sensitive instrument than the currently available 100-m class of radio telescopes.

In Table 1, we also include power-law spectral indices fitted for another seven objects with spectra containing flux measurements at only two frequencies (PSRs J1723−3659, J1739−3023, J1744−3130, J1751−3323, J1835−1020, J1842−0905 and J1901+0510). For obvious reasons, we did not conduct any fitting procedure for pulsars with flux density measured at only one frequency.

It must be remembered that almost all the above pulsars (with the only exceptions being PSRs B1811+40 and B1916+14) are objects with relatively high DMs. Therefore, using the standard pulsar flux measurement methods for these objects can cause erroneous results, especially when the observations are conducted at low observing frequencies where the pulsars are significantly affected by scattering. This typically occurs when the scattering tail is long enough to be a significant fraction of the pulsar period. In such cases, we might overestimate the off-pulse level, which in turn would lead to an underestimate of the pulsar flux density.

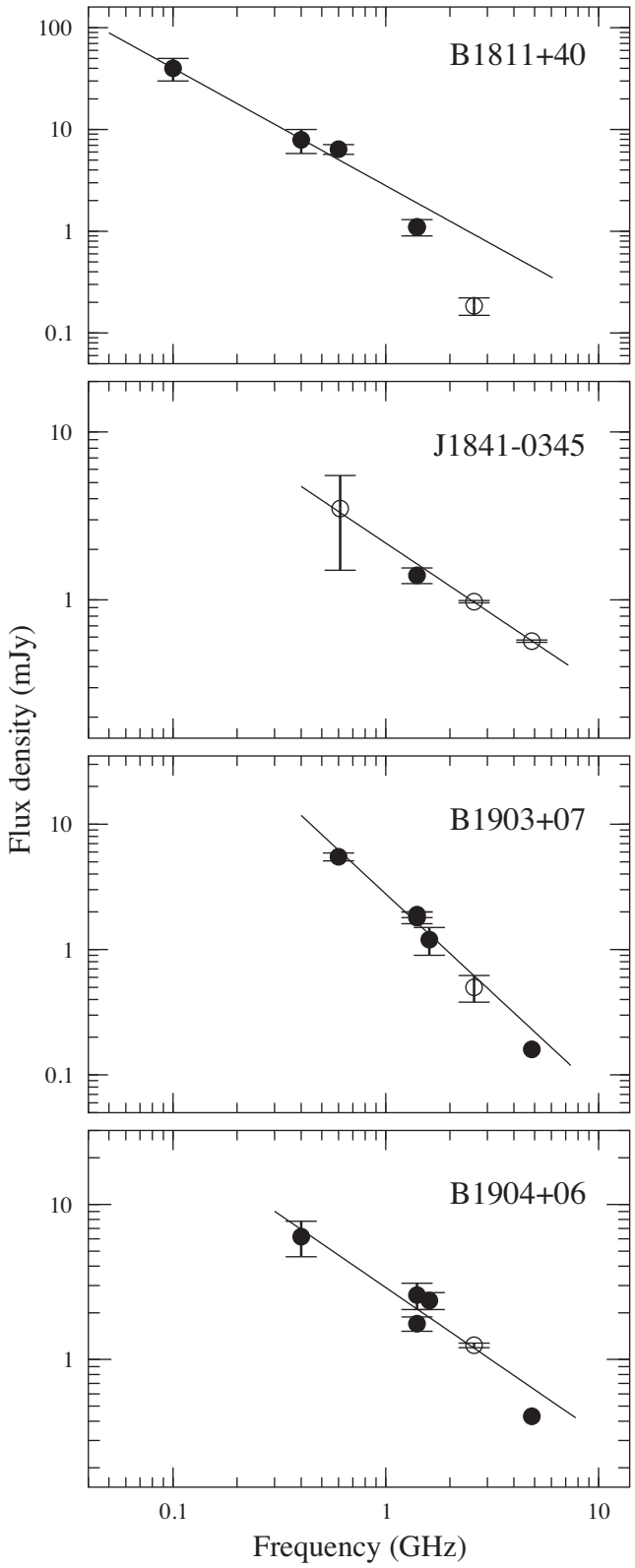

Figure 5. Radio spectra of four pulsars: PSRs B1811+40, J1841−0345, B1903+07 and B1904+06. Open circles denote our observations conducted in 2010 (610 MHz) and 2012 (2.6 and 4.85 GHz), whereas the black dots denote previously published data. The straight lines represent our fits to the data using a power-law function. The resulting spectral indices are presented in Table 1.

4 SUMMARY AND DISCUSSION

In this paper, we report two newly identified GPS pulsars, PSR J1740+1000 and PSR J1852−0635. We also present the spectra for 17 other pulsars, 13 of which are constructed for the first time. Among these, three sources can be considered as good candidates for GPS pulsars. Both the newly identified GPS pulsars are relatively young objects (114 kyr for PSR J1740+1000 and 567 kyr for PSR J1852−0635), which is a common characteristic for other known GPS pulsars. We have to note that PSR J1740+1000 is the first object to exhibit this phenomenon that has a low DM (24 pc cm^{-3}).

For PSR J1740+1000, we present the spectrum over a wide frequency range, which is an improvement compared with that previously published (Kijak et al. 2011b). The new spectrum still contains the flux measurement at 1170 MHz (see Fig. 1), which is unusually low compared to measurements at nearby frequencies. We consider it to be unreliable and we have excluded it from the spectral fitting procedure. The reason for this might be interstellar scintillations (as suggested in the discovery paper, McLaughlin, Arzoumanian & Cordes 2000), and we plan to address this issue with future observations near the frequency of 1 GHz. For the other new GPS pulsars, we only want to mention that the 1.4-GHz measurement (full circle in Fig. 2) is also slightly lower than the shape of the spectra (based on our data) would suggest. This measurement was obtained by Hobbs et al. (2004) and published in the Parkes discovery paper.

For the majority of the remaining pulsars, we obtained spectral indices that range from +0.3 to −2.0. Six of these can be considered to indicate flat spectra ($\xi > -1.0$). From our sample, we have selected three good GPS candidates. One of these sources is PSR J1705−3950, with the spectral index $\xi = +0.3$ based on observations made at two frequencies only (see Fig. 4). Because of its low declination, we were unable to obtain flux measurements at high frequencies using the Effelsberg radio telescope; such measurements would be possible only using Australian telescopes. The other two candidates, PSR J1812−2102 and J1834−0731, show typical spectra at high frequencies, but the flux-density upper limits we obtained at 610 MHz suggest that the spectra deviate from a simple power law, which might be an indication of possible GPS behaviour.

4.1 GPS pulsars

Summarizing, after the addition of the two new identifications presented here, we now have 11 GPS pulsars known. This number includes six objects presented in Kijak et al. (2011a), two radio magnetars (Kijak et al. 2013) and PSR J2007+2722 presented by Allen et al. (2013). This will definitely improve the statistics, which is important when trying to make reliable conclusions about the general properties of this class of objects (both pulsars and radio magnetars). However, the still relatively small sample of GPS pulsars, and with no direct correlation between spectra shapes and physical parameters (internal or external) that could affect the radiation properties, implies a still somewhat limited understanding of the properties of these objects as a group. Thus, successful searches for more GPS pulsars and low-frequency flux measurements in radio pulsars are very important.

The first of the new GPS pulsars presented here, PSR J1740+1000, was discovered in an Arecibo survey (McLaughlin et al. 2000) and was reported to have an unusually high positive spectral index of 0.9 (McLaughlin et al. 2002), which made it a good candidate object. The new observations indeed appear to be sufficient to identify the PSR J1740+1000 spectrum as a GPS

type. The object is very interesting from several points of view. *XMM–Newton* observations have revealed the existence of a PWN around the pulsar with a complex morphology (very extended pulsar tail; Kargaltsev et al. 2008). Later, Kargaltsev et al. (2012) reported absorption features in the X-ray spectrum of this ordinary rotation-powered radio pulsar and concluded that some of these features, thought to be unusual in neutron star spectra, are probably more common than earlier expected. They believe that their findings bridge the gap between the spectra of pulsars and other, more exotic neutron stars, such as X-ray dim isolated neutron stars (XDINSs), central compact objects (CCOs) and rotating radio transients (RRATs). PSR J1740+1000 was also considered by Romani et al. (2011) as a candidate subluminous γ-ray pulsar. Additionally, PSR J1740+1000 reveals a new aspect of pulsars with GPS: with a DM of 24 pc cm^{-3} (which, along this line of sight, corresponds to a distance of 1.2 kpc; Cordes & Lazio (2002)), it is much closer to us than other objects of this type.

Because of the high DMs of the GPS pulsars that were presented by Kijak et al. (2011a,b), it has been suspected that a high DM might have an important role to play in producing the GPS feature in radio pulsar spectra. However, with the recent GPS identifications reported here, it looks more likely that the effect might be related more to the environmental conditions in the close vicinity of these objects, rather than to the value of the DM. If this is the case, then the apparent observational trend for GPS pulsars to prefer higher DM values might be a pure selection effect. Because the GPS phenomenon is a rare occurrence, it is obvious that the chance of finding such objects increases with the size of the volume searched. However, this does not exclude the possibility of finding such objects at relatively low distances.

The case of PSR B1259−63 shows that the GPS feature observed in the spectrum can be caused by the absorption effects in the near vicinity of the pulsar (Kijak et al. 2011a, 2013). Our results for PSR J1740+1000 definitely support this idea, because it is another object with a peculiar environment, which makes it very similar to other GPS pulsars and magnetars.

An alternative mechanism, the flux dilution (which is caused by anomalous scattering), might also lead to a decrease of energy at lower frequencies, and hence it might change the appearance of pulsar radio spectra (J. Cordes, private communication). However, it would be difficult to use this to explain the case of PSR J1740+1000, which is a relatively nearby source and hence likely to be less affected by strong scattering effects.

5 CONCLUSIONS

In their recent statistical study, Bates et al. (2013) concluded that GPS sources might possibly constitute up to 10 per cent of the whole pulsar population, which could add up to as many as 200 objects. We believe that the currently small size of the GPS pulsar sample does not come from the fact that they are a rare phenomenon, but rather from our limited knowledge of pulsar spectra in general, especially at frequencies below 1 GHz.

The GPS phenomenon in radio magnetars along with the first low-DM GPS pulsar reported here lead us to revisit our criteria of selecting candidate GPS sources. In future searches, we would focus on sources with an interesting (or extreme) environment rather than those with a high DM. This would make the objects with PWNs/SNRs found in high-energy observations excellent GPS pulsar candidates. Vice versa, the sources with identified GPS would be good targets for high-energy observations.

Low-frequency flux-density measurements, which are crucial in the search for new GPS pulsars, can be difficult (or sometimes impossible) to conduct in the traditional way because of some of the known effects of the interstellar medium. Thus, we are able to determine pulsar flux densities using the standard on-and-off pulse energy estimates only when the scattering time is small enough. Many of the candidates for GPS pulsars have very high DMs and at lower frequencies they are not observable using regular pulsar observations, because of the extreme scattering that can smear their emission over the entire rotational period. This makes the observed radiation unpulsed (in extreme cases), or at least distorts the profile baseline to a degree that negates the standard means of making the flux-density measurement. For these cases, the only way to determine the pulsar flux is to use interferometric continuum imaging techniques (e.g. Kouwenhoven 2000). Thus, the interferometric imaging technique is important in these cases, providing an alternative for typical pulsar observations and making possible the verification of GPS, especially in the case of strong pulse scatter broadening (Lewandowski et al. 2013).

ACKNOWLEDGEMENTS

We thank the staff of the GMRT who have made our observations possible. The GMRT is run by the National Centre for Radio Astrophysics of the Tata Institute of Fundamental Research. This work is partially based on observations with the 100-m telescope of the Max-Planck-Institut für Radioastronomie (MPIfR) at Effelsberg. This research was partially supported by the grants DEC-2012/05/B/ST9/03924 and DEC-2013/09/B/ST9/02177 of the Polish National Science Centre. MD was a scholar within Submeasure 8.2.2 Regional Innovation Strategies, Measure 8.2 Transfer of knowledge, Priority VIII Regional human resources for the economy Human Capital Operational Programme co-financed by the European Social Fund and state budget. The research leading to these results has received funding from the European Commission Seventh Framework Programme (FP/2007-2013) under grant agreement No 283393 (RadioNet3).

REFERENCES

Allen B. et al., 2013, ApJ, 773, 91
Bates S. D., Lorimer D. R., Verbiest J. P. W., 2013, MNRAS, 431, 1352
Connors T. W., Johnston S., Manchester R. N., McConnell D., 2002, MNRAS, 336, 1201
Cordes J. M., Lazio T. J. W., 2002, preprint (astro-ph/0207156)
Gupta Y., 2000, in Kramer M., Wex N., Wielebinski R., eds, ASP Conf. Ser. Vol. 202, Pulsar Astronomy – 2000 and Beyond. Astron. Soc. Pac., San Francisco, p. 539
Hobbs G. et al., 2004, MNRAS, 352, 1439
Jessner A., 1996, in vant Klooster C. G. M., van Ardenne A., eds, Workshop on Large Antennas in Radio Astronomy. ESTEC, Noordwijk, p. 185
Johnston S., Manchester R. N., McConnell D., Campbell-Wilson D., 1999, MNRAS, 302, 277
Johnston S., Ball L., Wang N., Manchester R. N., 2005, MNRAS, 358, 1069
Kargaltsev O., Misanovic Z., Pavlov G. G., Wong J. A., Garmire G. P., 2008, ApJ, 684, 542
Kargaltsev O., Durant M., Misanovic Z., Pavlov G. G., 2012, Science, 337, 946
Kijak J., Gupta Y., Krzeszowski K., 2007, A&A, 462, 699
Kijak J., Dembska M., Lewandowski W., Melikidze G., Sendyk M., 2011a, MNRAS, 418, L114
Kijak J., Lewandowski W., Maron O., Gupta Y., Jessner A., 2011b, A&A, 531, A16

Kijak J., Lewandowski W., Bhattacharyya B., Gupta Y., 2011c, in Burgay M., D'Amico N., Esposito P., Pellizzoni A., Possenti A., eds, AIP Conf. Ser. Vol. 1357, Proc. Radio Pulsars: An Astrophysical Key to Unlock the Secrets of the Universe. American Institute of Physics, New York, p. 299
Kijak J., Tarczewski L., Lewandowski W., Melikidze G., 2013, ApJ, 772, 29
Kouwenhoven M. L. A., 2000, A&AS, 145, 243
Kuzmin A. D., Losovsky B. Ya., 2001, A&A, 368, 230
Lewandowski W., Dembska M., Kijak J., Kowalinska M., 2013, MNRAS, 434, 69
Löhmer O., Jessner A., Kramer M., Wielebinski R., Maron O., 2008, A&A, 480, 623
Lorimer D. R., Yates J. A., Lyne A. G., Gould D. M., 1995, MNRAS, 273, 411
McLaughlin M. A., Arzoumanian Z., Cordes J. M., 2000, in Kramer M., Wex N., Wielebinski R., eds, ASP Conf. Ser. Vol. 2002, Pulsar Astronomy – 2000 and Beyond. Astron. Soc. Pac., San Francisco, p. 41
McLaughlin M. A., Arzoumanian Z., Cordes J. M., Backer D. C., Lommen A. N., Lorimer D. R., Zepka A. F., 2002, ApJ, 564, 333
Manchester R. N., Hobbs G., Teoh A., Hobbs M., 2005, AJ, 129, 1993
Maron O., Kijak J., Kramer M., Wielebinski R., 2000, A&A,147, 195
Romani R. W., Kerr M., Craig H. A., Johnston S., Cognard I., Smith D. A., 2011, ApJ, 738, 114
Sieber W., 1973, A&AS, 28, 237

APPENDIX A: PULSE PROFILES AND WIDTHS

In this appendix, we present pulse profiles for the observed pulsars collected during our observing projects and the width measurements of the profiles.

Fig A1 shows the pulse profiles, acquired with both the GMRT (at 610 and 1170 MHz) and the Effelsberg telescope (at 2600, 4850 and 8350 MHz). We used the profiles to calculate the flux densities presented in Table 1. The flux-density values on the *y*-axes are expressed in arbitrary units.

The measurements of the pulse width are listed in Table A1.

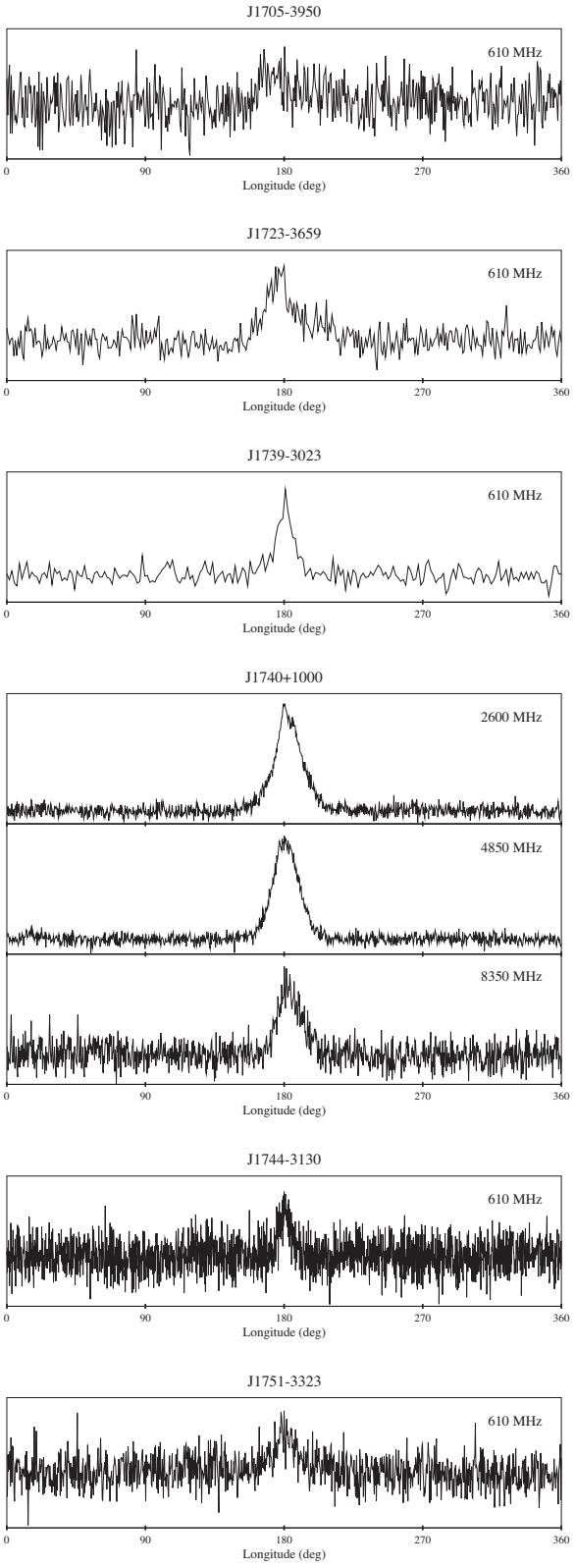

Figure A1. Pulsar profiles; vertical axes present the flux-density values in arbitrary units.

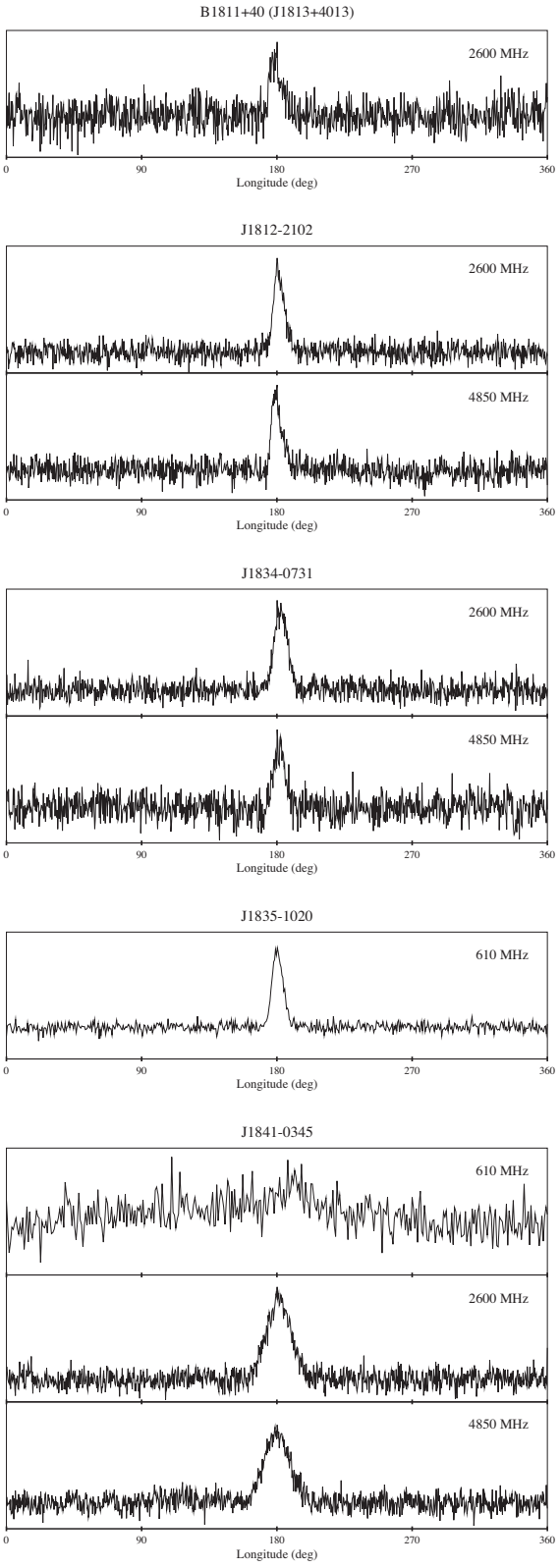

Figure A1. – *continued*

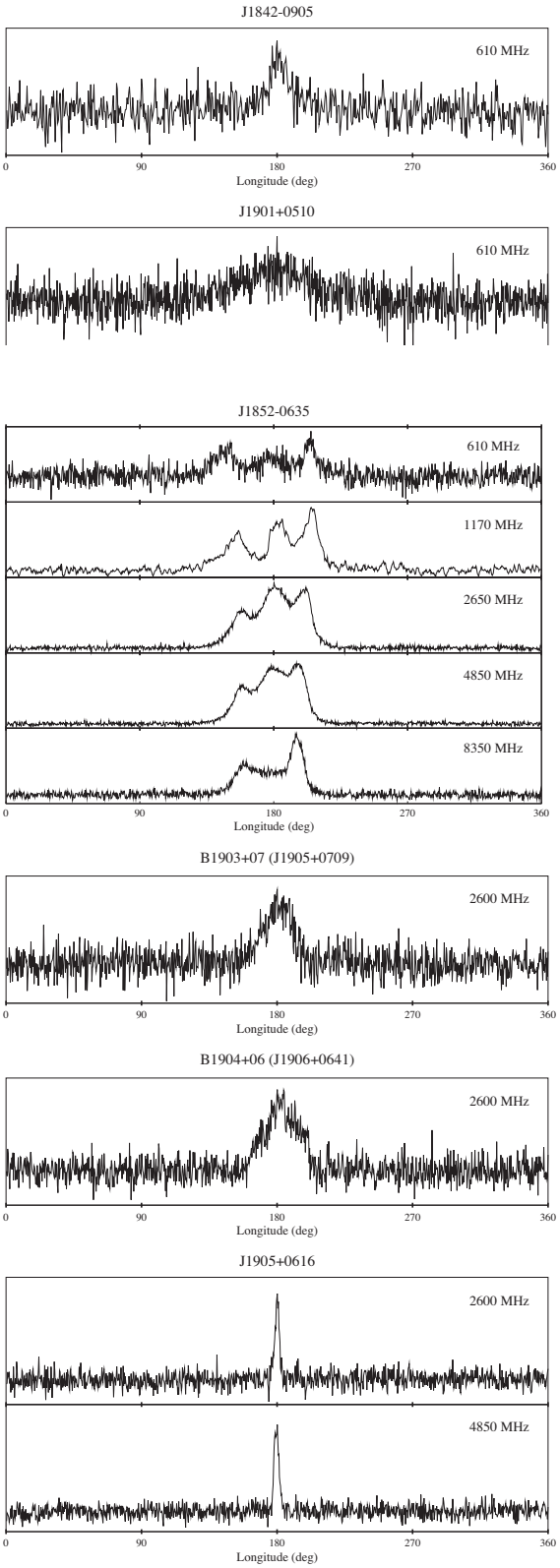

Figure A1. – *continued*

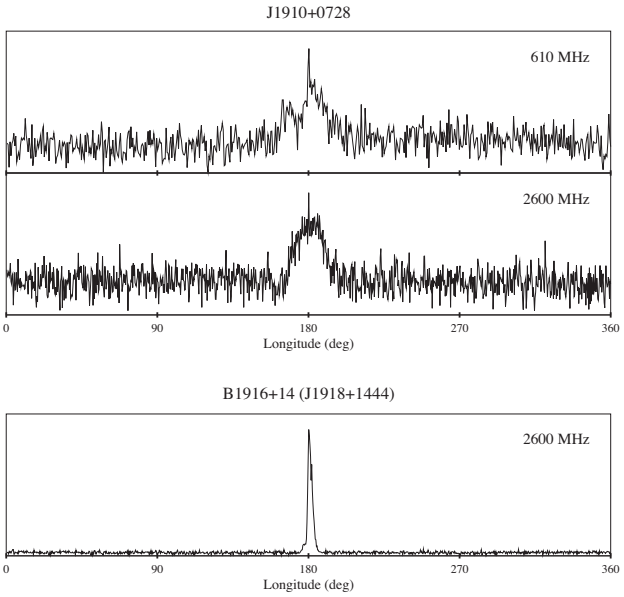

Figure A1. – *continued*

Table A1. Pulse widths for observed pulsars.

Pulsar	Frequency (MHz)	W_{10} (deg)	W_{50} (deg)
J1705−3905	610	69.90	38.30
J1723−3659	610	42.20	23.10
J1739−3023	610	23.80	13.10
J1740+1000	2600	37.30	20.40
	4850	36.30	19.30
	8350	33.10	19.00
J1744−3130	610	17.50	9.58
J1751−3323	610	30.80	16.90
B1811+40	2600	16.90	8.88
J1812−2102	2600	15.50	8.49
	4850	13.10	7.16
J1834−0731	2600	17.20	9.42
	4850	16.60	9.08
J1835−1020	610	15.50	8.52
J1841−0345	610	39.30	21.50
	2600	35.40	19.40
	4850	35.40	19.40
J1842−0905	610	25.20	13.80
J1852−0635	610	93.30	25.70
	1170	94.70	12.70
	2600	70.40	37.40
	4850	64.80	37.40
	8350	59.60	11.50
J1901+0510	610	111.00	61.00
B1903+07	2600	37.40	20.50
B1904+06	2600	49.40	27.10
J1905+0616	2600	6.76	3.71
	4850	6.77	3.72
J1910+0728	610	46.10	25.30
	2600	32.50	17.80
B1916+14	2600	5.70	3.13

This paper has been typeset from a TEX/LATEX file prepared by the author.